Thermoresponsive Complex Coacervate-Based Underwater Adhesive

Marco Dompé, Francisco Cedano-serrano, Olaf Heckert, Nicoline J van den Heuvel, Jasper van Der Gucht, Yvette Tran, Dominique Hourdet, Costantino Creton, Marleen Kamperman

Thermoresponsive Complex Coacervate-Based Underwater Adhesive

*Marco Dompé, Francisco J. Cedano-Serrano, Olaf Heckert, Nicoline van den Heuvel, Jasper van der Gucht, Yvette Tran, Dominique Hourdet, Costantino Creton, and Marleen Kamperman**

Sandcastle worms have developed protein-based adhesives, which they use to construct protective tubes from sand grains and shell bits. A key element in the adhesive delivery is the formation of a fluidic complex coacervate phase. After delivery, the adhesive transforms into a solid upon an external trigger. In this work, a fully synthetic in situ setting adhesive based on complex coacervation is reported by mimicking the main features of the sandcastle worm's glue. The adhesive consists of oppositely charged polyelectrolytes grafted with thermoresponsive poly(*N*-isopropylacrylamide) (PNIPAM) chains and starts out as a fluid complex coacervate that can be injected at room temperature. Upon increasing the temperature above the lower critical solution temperature of PNIPAM, the complex coacervate transitions into a nonflowing hydrogel while preserving its volume—the water content in the material stays constant. The adhesive functions in the presence of water and bonds to different surfaces regardless of their charge. This type of adhesive avoids many of the problems of current underwater adhesives and may be useful to bond biological tissues.

Underwater adhesion is technically challenging, because the performance of most adhesives is compromised by the presence of water, which eventually leads to bond failure.[1] The challenge of developing a fully functional underwater adhesive has been successfully overcome by several aquatic organisms, such as mussels, sandcastle worms, and barnacles, which are able to bond dissimilar materials together underwater using protein-based adhesives.[1–4] A phenomenon which is believed to play a fundamental role in the adhesive delivery is complex coacervation, which is an associative liquid–liquid phase separation of oppositely charged polyelectrolytes in solution.[5,6] Complex coacervates are particularly suitable for underwater adhesion, because of their fluid-like, yet water-immiscible properties[7,8] and good wettability.[9] In natural systems, after establishing molecular contact upon delivery, the complex coacervate liquid transforms into a solid material by the introduction of covalent or strong noncovalent interactions activated by a change in environmental conditions (e.g., higher pH in seawater, exposure to oxygen).[10] This principle has been mimicked in synthetic systems by designing polyelectrolyte material systems either responsive to a particular trigger (pH,[11–13] ionic strength,[14,15] solvent[16]) or toughening via a crosslinking reaction.[11,17,18] In this work a new temperature-triggered setting mechanism is introduced in a fully synthetic polyelectrolyte adhesive by grafting thermoresponsive poly(*N*-isopropylacrylamide) (PNIPAM) chains on oppositely charged polyelectrolyte backbones (**Figure 1**A).

Although reports of injectable hydrogels that can exhibit a temperature-dependent sol–gel transition can be found in literature,[19,20] the combination of complex coacervation with thermoresponsive domains to solidify the physical network results in a material system that has not yet been explored, which is expected to have key advantages for underwater adhesion: 1) Low viscosity to ensure precise and controlled delivery (e.g., via a syringe with needle).[15] 2) Easy manipulation in wet environments due to immiscibility of complex coacervates with water,[8] ensuring that the adhesive remains at the application site during setting. 3) Adhesion to diverse surfaces, because of the self-adjustable nature of the system. That means that depending on the target surface, different features (cationic, anionic, or hydrophobic) will be exposed to the surface.[21] 4) Effective in the presence of water, as no chemical reaction with

M. Dompé, O. Heckert, N. van den Heuvel, Prof. J. van der Gucht, Prof. M. Kamperman
Laboratory of Physical Chemistry and Soft Matter
Wageningen University & Research
Stippeneng 4, 6708 WE Wageningen, The Netherlands
E-mail: marleen.kamperman@rug.nl
F. J. Cedano-Serrano, Prof. Y. Tran, Prof. D. Hourdet, Prof. C. Creton
Soft Matter Sciences and Engineering
ESPCI Paris
PSL University
Sorbonne University
CNRS, F-75005 Paris, France
Prof. M. Kamperman
Polymer Science
Zernike Institute for Advanced Materials
University of Groningen
Nijenborgh 4, 9747 AG Groningen, The Netherlands

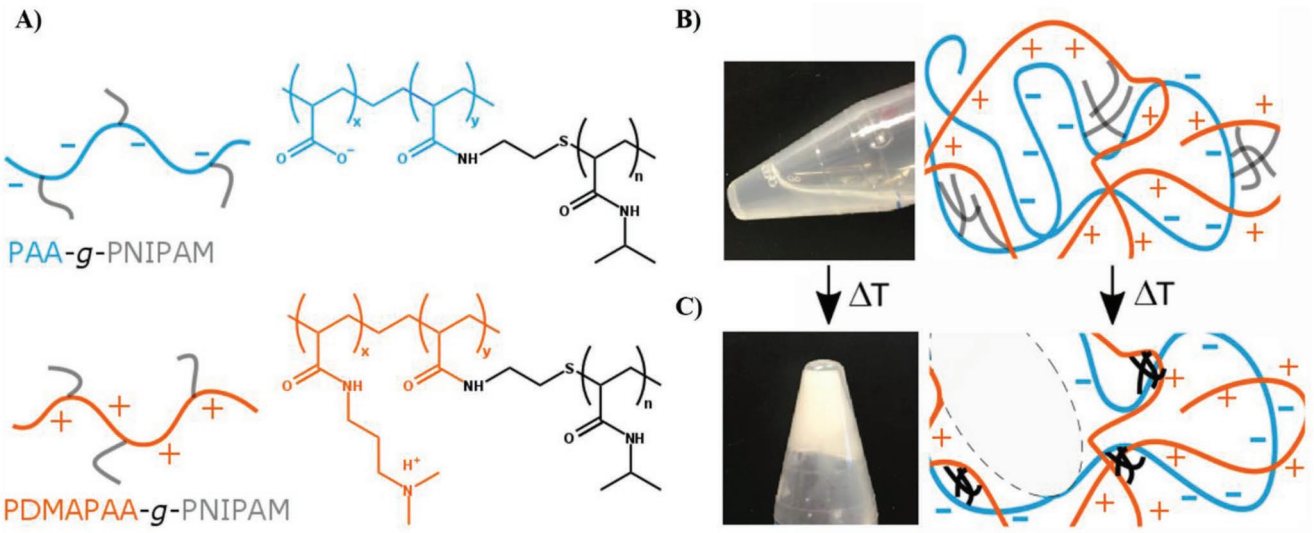

Figure 1. Composition and temperature responsiveness of the complex coacervate phase. A) Molecular structure of PAA-*g*-PNIPAM and PDMAPAA-*g*-PNIPAM. B) Picture and schematic representation of the complex coacervate structure below the LCST. C) Picture and schematic representation of the solidification triggered by increasing the temperature above PNIPAM LCST.

water or functional groups at the tissue surface is required, and thus can be injected through a fluid without being compromised. 5) In situ setting in the order of seconds or minutes with limited swelling. The liquid-to-solid transition is activated by a temperature gradient,[22] without the introduction of any chemical crosslinker—a feature required for thermoresponsive injectable hydrogels developed so far,[19,20] and can be tuned further by pH and salt concentration of the surrounding medium. 6) Controlled cohesive properties: the final material is held together by noncovalent ionic and hydrophobic interactions with a variety of bond strengths. Strong bonds may act as permanent crosslinks, imparting elasticity, whereas weak bonds can reversibly break and re-form, thereby dissipating energy and increasing the toughness.

Figure 1 schematically illustrates the composition, the morphological features, and the temperature response of the adhesive system. The adhesive starts out as a fluid complex coacervate obtained by mixing two oppositely charged graft copolymer solutions, namely poly(acrylic acid)-*grafted*-poly(*N*-isopropylacrylamide) (PAA-*g*-PNIPAM) and poly(dimethylaminopropyl acrylamide)-*grafted*-poly(*N*-isopropylacrylamide) (PDMAPAA-*g*-PNIPAM) (Figure 1A). The anionic polymer, PAA-*g*-PNIPAM ($M_n \approx 400$ kg mol^{-1}), was synthesized using a "grafting to" reaction, i.e., attaching PNIPAM side chains ($M_n \approx 5.5$ kg mol^{-1}) onto a PAA backbone ($M_n \approx 200$ kg mol^{-1}) using a coupling reaction (Figure S1, Supporting Information).[23] The cationic polymer, PDMAPAA-*g*-PNIPAM ($M_n \approx 250$ kg mol^{-1}), was obtained by copolymerizing DMAPAA monomers with PNIPAM macromonomers ($M_n \approx 5.5$ kg mol^{-1}), i.e., PNIPAM chains with a polymerizable end-group (Figure S3, Supporting Information), using a "grafting through" polymerization process (Figure S5, Supporting Information).[24] The synthesis procedures and the characterization for both polymers are described in Figures S1–S6 in the Supporting Information. In both polyelectrolytes, the molar ratio between charged monomers in the backbone and PNIPAM side chains is around 70:30 (Table S1, Supporting Information).

Complex coacervation strongly depends on solution conditions, such as pH, mixing ratio, and salt concentration. It is known that, in general, complexation is most effective when both polyelectrolytes carry the same number of charges.[8] To establish the point of charge neutrality and optimal complexation conditions, pH titrations and zeta potential experiments were performed (Figures S7–S10, Supporting Information). Based on the results of these experiments, the polyelectrolytes were mixed at pH 7.0 and at 1:1 stoichiometric ratio of chargeable units, to reach a total charged monomer concentration of 0.05 M. Salt concentration affects the strength and the relaxation dynamics of the ionic bonds and thereby the viscosity of the complex coacervate;[9] here the added sodium chloride (NaCl) concentration was set to 0.75 M, just below the critical salt concentration (threshold above which complexation is suppressed),[7,8] to obtain a low-viscosity fluid phase, the properties of which will be discussed in detail in the following.

To study the influence of the thermoresponsive PNIPAM grafts, complex coacervates were prepared at room temperature (RT, 20 °C) by mixing graft copolymer solutions (PAA-*g*-PNIPAM and PDMAPAA-*g*-PNIPAM) and homopolymer solutions (PAA and PDMAPAA). When heated above 35 °C the complex coacervates prepared from graft copolymer solutions, which were initially transparent and fluid-like, become white and solid-like (Figure 1B,C), unlike samples prepared from homopolymer solutions which remain transparent and liquid. This transition is attributed to the aggregation of PNIPAM side chains into microdomains which densify when the temperature is raised above the lower critical solution temperature (LCST),[25] leading to the formation of physical crosslinks in the material. The LCST is strongly affected by the ionic strength of the medium: because of the salting-out effect of NaCl,[26] the LCST at 0.75 M NaCl, detected by differential scanning calorimetry (DSC), is observed at ≈23 °C (Figure S11, Supporting Information), which is lower than typically observed in pure water, i.e., ≈32 °C. The liquid-to-solid transition is fully reversible, i.e.,

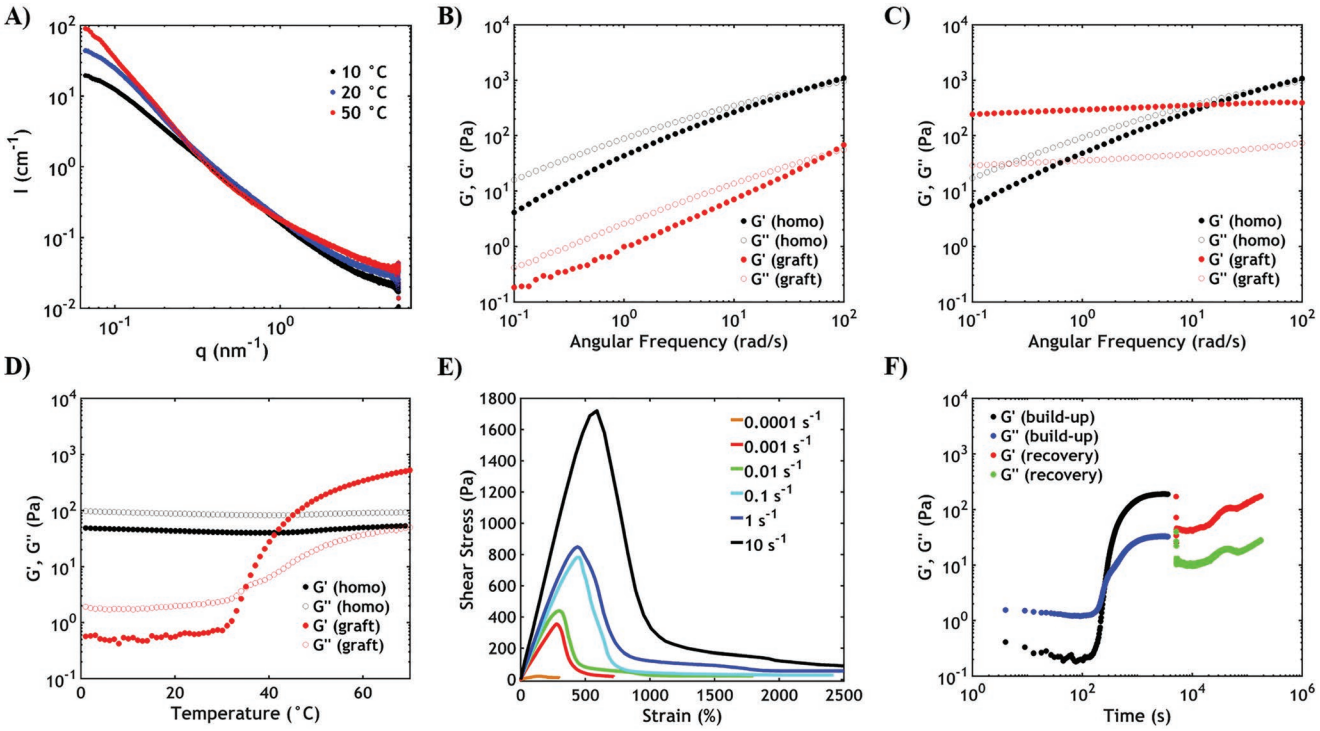

Figure 2. Morphological and mechanical behavior of the underwater adhesive system. A) SAXS profile for graft copolymer complex coacervates obtained at different temperatures. B,C) Frequency sweeps performed at 20 °C (B) and at 50 °C (C), and D) temperature sweeps performed at 1 rad s^{-1} for homopolymer and graft copolymer complex coacervates. E) Shear start-up experiments at different shear rates and F) moduli build-up during the heating step and moduli recovery after failure for graft copolymer complex coacervates.

the material returns to the transparent and liquid state when cooled to 4 °C.

To investigate structural differences below and above the LCST, small-angle X-ray scattering (SAXS) analysis was performed. At high q (0.3–3 nm^{-1}, corresponding to length scales at which the conformation of single polymer chains is detected), the curves for both homopolymer (Figure S12, Supporting Information) and graft copolymer (**Figure 2**A) complex coacervates show a similar slope ($I \approx q^{-1.7}$) regardless of temperature. This suggests that the conformation of the individual chains is similar in both graft and homopolymer systems and does not change much as a function of temperature. More specifically, this q-dependence indicates that the polymer chains attain a self-avoiding random walk conformation, behaving nearly as in a semidilute polyelectrolyte solution.[27] At larger length scales (q-range 0.06–0.3 nm^{-1}), an upturn is detected, whose intensity increases as a function of temperature and which is not visible in complex coacervates prepared from homopolymers. This upturn is ascribed to the increased nonsolubility of PNIPAM domains (with dimensions of tens of nanometers, according to the observed q-range) and the decreased compatibility between PNIPAM and the complex coacervate phase. The absence of a well-defined peak might indicate that the generated PNIPAM domains are polydisperse. The upturn is already observed at temperatures below the LCST indicating that PNIPAM chains cluster already at RT. The heterogeneity of the material is apparent even at the micrometer-scale, as evidenced by optical microscopy images (Figure S13, Supporting Information): the presence of domains, whose size increase from 10 to 30–50 µm by heating from 20 to 50 °C, can clearly be detected.

Upon collapse of the PNIPAM chains, the domains are expected to shrink and to expel water, as observed in PNIPAM hydrogels.[28] However, no change in water content (≈91%) and volume is detected upon the liquid-to-solid transition (Table S2, Supporting Information). We speculate that the water expelled by PNIPAM is retained in pockets inside the complex coacervate phase, leading to the formation of a porous structure (Figure 1C).[5,29,30] The isochoric nature of the transition might be beneficial to the overall adhesive performance, since it would prevent both swelling, which can result in mechanical weakening,[20] and lubrication at the sample–probe interface, which would decrease the adhesion.[1] Moreover it would maintain the flexibility and stretchability of the material by keeping a relatively high amount of water within the complex coacervate phase.[31]

Rheological measurements were performed as a function of frequency and temperature in the linear regime (Figure S14, Supporting Information). At 20 °C, both complex coacervates prepared from homopolymer and graft copolymer solutions possess a fluid character with the storage modulus (G') crossing the loss modulus (G'') only at high frequencies (Figure 2B). In both systems, at 20 °C the chains slide along each other with transient electrostatic interactions, giving rise to sticky Rouse dynamics.[32] The crossover frequency (ω_c) is higher (≈70 rad s^{-1}) in graft copolymer coacervates as

compared to homopolymer complex coacervates (≈45 rad s^{-1}), while both moduli are lower over the whole frequency range. We attribute these differences to the higher water content in the PNIPAM containing systems (92% vs 83% in homopolymer complex coacervates), leading to a lower concentration of charged units (sticky points) and, as a consequence, shorter relaxation times τ ($\tau = 1/\omega_c$). The rheological data obtained at 50 °C show that in graft copolymer complex coacervates, contrary to homopolymer complex coacervates, both moduli increase and become nearly frequency independent, with G' exceeding G'' (Figure 2C). This indicates that the complex coacervate, upon the increase in temperature, turns into a soft elastic solid because of the slowing down of the PNIPAM chain dynamics in the domains, leading to the formation of physical crosslinks which strengthen the material.[33] The G' and G'' values are comparable, in order of magnitude, to the ones obtained for water solutions of graft copolymers with a neutral backbone (poly(*N*,*N*-dimethylacrylamide)) and PNIPAM side chains:[22] it is not surprising to detect similarities since at such a high salt concentration the charged units are almost completely screened and the few remaining ones are complexed with each other, so that the polyelectrolyte complex backbone is overall neutral. The observed phase transition is desirable for injectable underwater adhesives, which need to properly wet the surface upon application, yet sustain stress to prevent debonding.[34] At low temperatures, PNIPAM allows higher water retention, making the material more liquid-like and providing good contact with the surface, while increasing the temperature reinforces the material.

In order to accurately detect the liquid-to-solid transition, temperature sweeps were performed on the complex coacervates, heating the sample from 0 to 70 °C (Figure 2D). While the moduli of homopolymer complex coacervates are temperature independent, both G' and G'' in graft copolymer complex coacervates start increasing above 26 °C, with the transition occurring at 34 °C, where the moduli crossover is detected.

In order to study the material performance at high deformations, shear start-up experiments were performed at 50 °C over a wide range of shear rates (Figure 2E). At low strains, the material shows features of an elastic solid: a linear dependence is observed between stress (σ) and strain (ε). The stress then rises to a maximum before decreasing to a low value: the sharp decrease in stress indicates fracture by failure of the physical network. Both stress and strain at failure increase linearly with the logarithm of the applied shear rate (Figure S16, Supporting Information), in line with earlier work on fracture of physical gels network, which was explained using an activated bond rupture model.[35] Since failure of the network is observed in every measurement, the relaxation time (τ) of the PNIPAM domains is longer than the inverse of the lowest shear rate applied ($\tau > 10^4$ s).

Furthermore, the recovery of the oscillatory moduli after failure was studied at 50 °C. Figure 2F shows the moduli development during a temperature sweep. After a shear start-up experiment, the moduli decrease drastically as a consequence of failure of the network. However, the moduli start to regenerate after rupture and, after 48 h, they almost recover their original values (91% for G', 86% for G''). This means that, after failure, the broken physical crosslinks can partially reform at the fracture interface. However, it is necessary to add a cooling step (RT for 1 h) after failure to recover the nonlinear properties, i.e., the fracture strength (Figures S17 and S18, Supporting Information). This suggests that a higher mobility of the PNIPAM chains is required to recreate physical bonds across the previously broken interface.

Underwater adhesion experiments were conducted on complex coacervates prepared both from homopolymer and graft copolymer solutions using a probe-tack test performed completely underwater with the setup developed by Sudre et al.[36] (**Figure 3**A). The water solution present in the measurement chamber was prepared at the same pH and salt concentration as that of the analyzed samples, so that the setting mechanism observed could only be ascribed to a temperature difference.

Contact was made at 20 °C between the fluid complex coacervate and a negatively charged poly(acrylic acid) (PAA) hydrogel thin film (underwater thickness = 257 nm),[37] attached on the probe surface, until a fixed thickness of 0.5 mm was reached. The PAA functionalized probe was then pulled off either at 20 or 50 °C at a fixed velocity of 100 μm s^{-1} (corresponding to an initial strain rate of 0.2 s^{-1} and to a fixed thickness of 0.5 mm). Complex coacervates prepared from homopolymer solutions at 0.75 M NaCl can be easily stretched to high strain values but cannot sustain any stress, both at 20 and 50 °C, due to their viscous fluid character (Figure S19, Supporting Information). A similar trend is observed when probing the performance of complex coacervates prepared from graft copolymer solutions at 20 °C at 0.75 M NaCl, providing low values of work of adhesion ($W_{adh} \approx 0.02$ J m^{-2}). When detachment is performed at 50 °C, the formation of PNIPAM physical crosslinks strengthens the adhesive, resulting in an increase in work of adhesion by two orders of magnitude in ($W_{adh} = 1.6$ J m^{-2}) (Figure 3B; Figure S22, Supporting Information). At high strain, the formation of filaments is observed (Figure 3C); however, the stress they can sustain is close to the noise level of the apparatus so that it is not trivial to detect their presence by just observing the adhesion plots. At the end of the test, fibrils break leaving residues of material on the probe surface. This indicates that the mode of failure is cohesive. The same result is obtained when making contact underwater or in air, meaning that good contact with the PAA hydrogel surface can always be achieved, also through water (Figure S21, Supporting Information). This would not be feasible with glues that cure upon reaction with water, like conventional cyanoacrylates, or with water solutions of thermoresponsive graft copolymers bearing neutral backbones[22] since they would disperse in the environment.

It is important to tune the ionic strength to obtain optimal properties: if the ionic strength is below a certain threshold, the complex coacervate possesses a solid character already at RT because of the increased strength of the electrostatic interactions between the oppositely charged backbones (Figure S15, Supporting Information). A fluidic character is not only important to preserve the injectability of the glue, but also greatly influences the adhesive performance. When testing the underwater adhesive properties of graft copolymer complex coacervates prepared at a lower salt concentration (0.5 M NaCl), the recorded W_{adh} is drastically decreased (0.3 J m^{-2}) (Figures S23 and S24, Supporting Information). The reduced mobility of

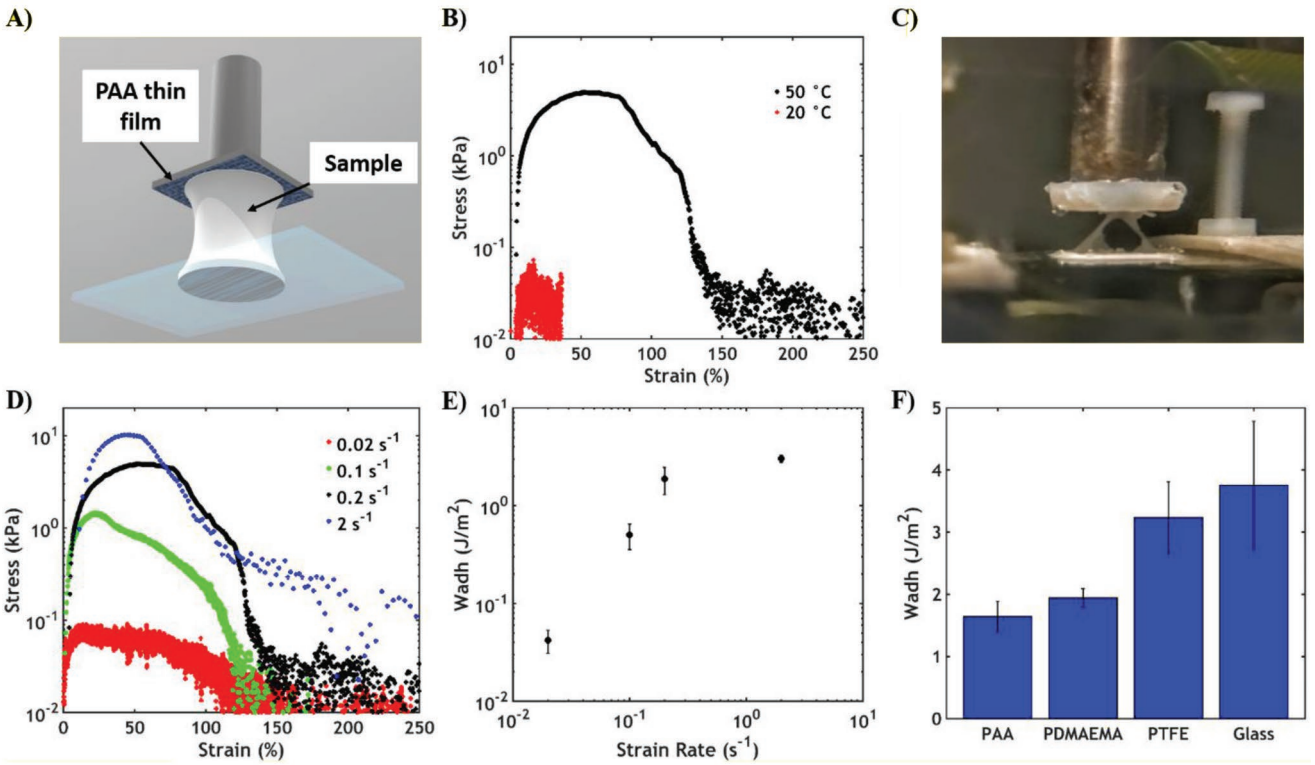

Figure 3. Underwater adhesion experiments. A) Schematics of the probe-tack test performed underwater. The complex coacervate is loaded on a glass slide and contact with a charged probe surface is made underwater at 20 °C. The detachment is then performed either at 20 or 50 °C. B) Effect of temperature on the adhesion performance. C) Formation of filaments at high strain. D,E) Effect of strain rate and F) type of surface on adhesion performance and on work of adhesion when the detachment is performed at 50 °C. Points represent the average work of adhesion and the error bars represent the standard deviation.

the polymer chains within the material may prohibit PNIPAM domains from forming, which explains this reduction in W_{adh}.

When performing the test at different strain rates, a trend similar to what was observed in the nonlinear rheology experiments and in other adhesion studies on viscoelastic materials[38] was detected. The stress peak and the work of adhesion increase as a function of detaching speed, indicating that at higher rates the system has insufficient time to relax the stress when probed, so that energy needs to be dissipated upon detachment (Figure 3D,E).

Another parameter that plays a key role in the adhesion performance is the interaction between the sample and the probe surface. The complex coacervate adheres strongly to both hydrophilic (glass) and hydrophobic surfaces (poly(tetrafluoroethylene), PTFE), providing higher W_{adh} values (W_{adh} on glass = 3.8 J m^{-2}, W_{adh} on PTFE = 3.2 J m^{-2}) than using the negatively charged PAA surface (Figure 3F). This versatility might be due to the presence of hydrophobic PNIPAM domains, which upon collapse repel water (providing good adhesion to hydrophobic surfaces), and, at the same time, to high water retention inside the material upon the phase transition (favoring adhesion to hydrophilic surfaces). The increase in W_{adh} compared to the experiments performed using the PAA thin film might be ascribed to a higher roughness of the PTFE and glass surfaces. The mode of failure is always cohesive.

A comparison with literature data is not straightforward due to differences in sample preparation and testing methodologies. Therefore, we limit the comparison to other adhesive systems tested with underwater probe-tack testing. The presented thermoresponsive complex coacervates show a much higher work of adhesion than standard commercial pressure sensitive adhesives (W_{adh} = 0.02–0.26 J m^{-2})[39] and a similar work of adhesion as other biomimetic underwater adhesives (W_{adh} = 0.75–6.5 J m^{-2}).[39–41] However, these materials either need to be solidified by an externally activated (UV-light) polymerization process or undergo gelation before application, while the system developed here sets in situ only by a change in environmental conditions, providing a key additional advantage for use as injectable adhesive.

The same probe-tack experiments were performed by using, as a probe, a positively charged brush, obtained by attaching poly(dimethylaminoethyl methacrylate) (PDMAEMA) chains to the probe surface,[42] and a similar work of adhesion (W_{adh} = 1.9 J m^{-2}) and probe-tack curve as with the negatively charged PAA surface were obtained (Figure 3F; Figure S27, Supporting Information). The complex coacervate contains an equal amount of positive and negative charges, possessing similar characteristics to the polyampholyte gels synthesized by Roy et al.[21] This class of materials most probably form ionic bonds with any charged surface, either positive or negative, because of a local polarization of the hydrogel at the interface when a charged countersurface is approached. In other words, electrostatic interactions forming between the probe surface and the complex coacervate can sustain an

adhesive stress while the thermoresponsive PNIPAM chains contribute a bulk dissipation mechanism to the overall adhesion performance.

In conclusion, a new proof of principle for underwater adhesion has been developed in this work. The results show that complex coacervation provides a promising delivery vehicle for underwater adhesives and that physical crosslinking of a complex coacervate results in a material system with interesting, largely unexplored properties.

Supporting Information

Supporting Information is available from the Wiley Online Library or from the author.

Acknowledgements

This project is part of the BioSmartTrainee Network. The project received funding from the European Union's Horizon 2020 research and innovation programme under the Marie Sklodowska-Curie grant agreement no. 642861. The authors acknowledge Ilse van Hees, Alexei Filippov, and Remco Fokkink for help in collecting SAXS data. The authors acknowledge Ugo Sidoli and Alla Synytska for providing the PDMAEMA brushes. The authors acknowledge Dr. Thomas Kodger for collecting optical microscopy images and for useful discussions. J.v.d.G. acknowledges the European Research Council for financial support (ERC Consolidator grant Softbreak).

Conflict of Interest

The authors declare no conflict of interest.

Keywords

complex coacervates, environmentally triggered phase transitions, lower critical solution temperature, poly(*N*-isopropylacrylamide), underwater adhesion

Received: December 19, 2018
Revised: March 5, 2019
Published online: March 29, 2019

[1] J. H. Waite, *Int. J. Adhes. Adhes.* **1987**, *7*, 9.
[2] G. Walker, *Mar. Biol.* **1970**, *7*, 239.
[3] J. H. Waite, N. H. Andersen, S. Jewhurst, C. Sun, *J. Adhes.* **2005**, *81*, 297.
[4] R. J. Stewart, J. C. Weaver, D. E. Morse, J. H. Waite, *J. Exp. Biol.* **2004**, *207*, 4727.
[5] R. J. Stewart, C. S. Wang, I. T. Song, J. P. Jones, *Adv. Colloid Interface Sci.* **2017**, *239*, 88.
[6] R. J. Stewart, C. S. Wang, H. Shao, *Adv. Colloid Interface Sci.* **2011**, *167*, 85.
[7] J. van der Gucht, E. Spruijt, M. Lemmers, M. A. Cohen Stuart, *J. Colloid Interface Sci.* **2011**, *361*, 407.
[8] E. Spruijt, A. H. Westphal, J. W. Borst, M. A. Cohen Stuart, J. van der Gucht, *Macromolecules* **2010**, *43*, 6476.
[9] E. Spruijt, J. Sprakel, M. A. Cohen Stuart, J. van der Gucht, *Soft Matter* **2010**, *6*, 172.
[10] A. H. Hofman, I. A. van Hees, J. Yang, M. Kamperman, *Adv. Mater.* **2018**, *30*, 1704640.
[11] H. Shao, R. J. Stewart, *Adv. Mater.* **2010**, *22*, 729.
[12] P. G. Lawrence, Y. Lapitsky, *Langmuir* **2015**, *31*, 1564.
[13] S. Seo, S. Das, P. J. Zalicki, R. Mirshafian, C. D. Eisenbach, J. N. Israelachvili, J. H. Waite, B. K. Ahn, *J. Am. Chem. Soc.* **2015**, *137*, 9214.
[14] Q. Wang, J. B. Schlenoff, *Macromolecules* **2014**, *47*, 3108.
[15] J. P. Jones, M. Sima, R. G. O'Hara, R. J. Stewart, *Adv. Healthcare Mater.* **2016**, *5*, 795.
[16] Q. Zhao, D. W. Lee, B. K. Ahn, S. Seo, Y. Kaufman, J. N. Israelachvili, J. H. Waite, *Nat. Mater.* **2016**, *15*, 407.
[17] B. K. Ahn, S. Das, R. Linstadt, Y. Kaufman, N. R. Martinez-Rodriguez, R. Mirshafian, E. Kesselman, Y. Talmon, B. H. Lipshutz, J. N. Israelachvili, J. H. Waite, *Nat. Commun.* **2015**, *6*, 8663.
[18] S. Kaur, G. M. Weerasekare, R. J. Stewart, *ACS Appl. Mater. Interfaces* **2011**, *3*, 941.
[19] Y. Lee, H. J. Chung, S. Yeo, C.-H. Ahn, H. Lee, P. B. Messersmith, T. G. Park, *Soft Matter* **2010**, *6*, 977.
[20] D. G. Barrett, G. G. Bushnell, P. B. Messersmith, *Adv. Healthcare Mater.* **2013**, *2*, 745.
[21] C. K. Roy, H. L. Guo, T. L. Sun, A. B. Ihsan, T. Kurokawa, M. Takahata, T. Nonoyama, T. Nakajima, J. P. Gong, *Adv. Mater.* **2015**, *27*, 7344.
[22] H. Guo, A. Brûlet, P. R. Rajamohanan, A. Marcellan, N. Sanson, D. Hourdet, *Polymer* **2015**, *60*, 164.
[23] A. Durand, D. Hourdet, *Polymer* **1999**, *40*, 4941.
[24] L. Petit, C. Karakasyan, N. Pantoustier, D. Hourdet, *Polymer* **2007**, *48*, 7098.
[25] M. Heskins, J. E. Guillet, *J. Macromol. Sci., Part A* **1968**, *2*, 1441.
[26] Y. Zhang, S. Furyk, D. E. Bergbreiter, P. S. Cremer, *J. Am. Chem. Soc.* **2005**, *127*, 14505.
[27] A. B. Marciel, S. Srivastava, M. V. Tirrell, *Soft Matter* **2018**, *14*, 2454.
[28] Y. Kaneko, R. Yoshida, K. Sakai, Y. Sakurai, T. Okano, *J. Membr. Sci.* **1995**, *101*, 13.
[29] C. H. Porcel, J. B. Schlenoff, *Biomacromolecules* **2009**, *10*, 2968.
[30] H. Guo, N. Sanson, A. Marcellan, D. Hourdet, *Macromolecules* **2016**, *49*, 9568.
[31] L. Han, K. Liu, M. Wang, K. Wang, L. Fang, H. Chen, J. Zhou, X. Lu, *Adv. Funct. Mater.* **2018**, *28*, 1704195.
[32] E. Spruijt, M. A. Cohen Stuart, J. van der Gucht, *Macromolecules* **2013**, *46*, 1633.
[33] J. Courtois, I. Baroudi, N. Nouvel, E. Degrandi, S. Pensec, G. Ducouret, C. Chanéac, L. Bouteiller, C. Creton, *Adv. Funct. Mater.* **2010**, *20*, 1803.
[34] C. Creton, *MRS Bull.* **2003**, *28*, 434.
[35] P. J. Skrzeszewska, J. Sprakel, F. A. de Wolf, R. Fokkink, M. A. Cohen Stuart, J. van der Gucht, *Macromolecules* **2010**, *43*, 3542.
[36] G. Sudre, L. Olanier, Y. Tran, D. Hourdet, C. Creton, *Soft Matter* **2012**, *8*, 8184.
[37] B. Chollet, M. Li, E. Martwong, B. Bresson, C. Fretigny, P. Tabeling, Y. Tran, *ACS Appl. Mater. Interfaces* **2016**, *8*, 11729.
[38] A. Ahagon, A. N. Gent, *J. Polym. Sci., Polym. Phys. Ed.* **1975**, *13*, 1285.
[39] S. K. Clancy, A. Sodano, D. J. Cunningham, S. S. Huang, P. J. Zalicki, S. Shin, B. K. Ahn, *Biomacromolecules* **2016**, *17*, 1869.
[40] M. Guvendiren, P. B. Messersmith, K. R. Shull, *Biomacromolecules* **2008**, *9*, 122.
[41] H. Chung, P. Glass, J. M. Pothen, M. Sitti, N. R. Washburn, *Biomacromolecules* **2011**, *12*, 342.
[42] C. Marschelke, I. Raguzin, A. Matura, A. Fery, A. Synytska, *Soft Matter* **2017**, *13*, 1074.